SOIL ORGANIC CARBON ASSESSMENT BY FIELD AND AIRBORNE SPECTROMETRY IN BARE CROPLANDS: ACCOUNTING FOR SOIL SURFACE ROUGHNESS

Paper published in Geoderma (ELSEVIER) and Available online 1st April 2014. Geoderma Volumes 226–227, August 2014, Pages 94–102, http://dx.doi.org/10.1016/j.geoderma.2014.02.015.

Antoine DENIS[*, a], *Antoine STEVENS* [b], *Bas van WESEMAEL*[b], *Thomas UDELHOVEN* [c] *Bernard TYCHON* [a]

a Department of Environmental Sciences and Management, Arlon Campus Environnement, University of Liège, 185, Avenue de Longwy, 6700 Arlon, Belgium
b Georges Lemaître Centre for Earth and Climate Research, Earth and Life Institute, Université catholique de Louvain, Place Pasteur, 3, 1348 Louvain-La-Neuve, Belgium
c Centre de Recherche Public Gabriel Lippmann, 162 av de la Faïencerie, 1511 Luxembourg, Grand Duchy of Luxembourg.
*Corresponding author:
Antoine DENIS, ULg Arlon Campus Environnement, Avenue de Longwy 185, 6700 Arlon, Belgium
Phone: +32 63 23 09 97
E-mail: Antoine.Denis@ulg.ac.be

ABSTRACT

Visible, Near and Short Wave Infrared (VNSWIR) diffuse reflectance spectroscopy (350 nm to 2500 nm) has been proven to be an efficient tool to determine the **Soil Organic Carbon (SOC) content**. SOC assessment (SOCa) is usually done by using calibration samples and multivariate models. However one of the major constraints of this technique, when used in field conditions is the **spatial variation in surface soil properties** (soil water content, roughness, vegetation residue) which induces a spectral variability not directly related to SOC and hence reduces the SOCa accuracy. This study focuses on the impact of **soil roughness** on SOCa by outdoor VIS-NIR-SWIR spectroscopy and is based on the assumption that soil roughness effect can be approximated by its related **shadowing effect**.

A **new method** for identifying and correcting the effect of soil shadow on reflectance spectra measured with an Analytical Spectral Devices (ASD) spectroradiometer and an Airborne Hyperspectral Sensor (AHS-160) on freshly tilled fields in the Grand Duchy of Luxembourg was elaborated and tested. This method is based on the shooting of soil vertical photographs in the visible spectrum and the derivation of a shadow correction factor resulting from the comparison of "reflectance" of shadowed and illuminated soil areas.

Moreover, the study of laboratory ASD reflectance of shadowed soil samples showed that the influence of shadow on reflectance varies according to wavelength. Consequently a correction factor in the entire [350 -2500 nm] spectral range was computed to translate this differential influence.

Our results showed that SOCa was improved by 27% for field spectral data and by 25% for airborne spectral data by correcting the effect of soil relative shadow. However, compared to simple mathematical treatment of the spectra (first derivative, etc) able to remove variation in soil albedo due to roughness, the proposed method, leads only to slightly more accurate SOCa.

Keywords: soil spectroscopy; soil organic carbon; soil roughness; soil shadow; image segmentation

---

VNSWIR: Visible, Near and Short Wave Infrared; **SOCa**: Soil Organic Carbon assessment; **ASD**: Analytical Spectral Devices; **AHS**: Airborne Hyperspectral Sensor; **soil RS**: soil Relative Shadow; **SZA**: Solar Zenith Angle

1. INTRODUCTION

The monitoring of soil attributes and their evolution over time as well as the development of pedological models rely on the availability of accurate and extensive soil data. The high spatial variability of soils arising from both local and global factors of soil formation requires generally collecting soil information from a very dense network of sites. Diffuse **reflectance spectroscopic techniques**, and in particular Visible, Near and Short Wave Infra Red (VNSWIR) spectroscopy (350 nm to 2500 nm), allows rapid sampling and instantaneous determination of many soil properties, at field and regional levels (in remote sensing mode). This technique can provide in a cost effective way the large quantity of spatial data required in soil monitoring or modelling studies like the monitoring of decline of soil organic matter in the topsoil.

Spectral libraries and multivariate modelling are often used to predict soil attributes of unknown samples. In the laboratory, such approach has proven to provide accurate determinations of SOC (Viscarra Rossel et al., 2006). When using the same approach, field spectroscopy and hyperspectral remote sensing, however, may fail to produce reliable and robust determinations due to uncontrolled measuring conditions and spatial variation in surface soil properties. According to Atzberger (2000), the **main factors affecting the soil reflectance** are soil water content, vegetation residues and surface roughness.

For the purpose of this study, field spectroscopic measurements were taken over bare and dry soils. Hence soil **roughness** remained the main disturbing factor and other influences have not been taken into consideration.

The effect of roughness on soil reflectance has been addressed in several studies. Arnfield (1975) showed that, for a relatively rough soil surface, soil albedo is generally lower than for a corresponding smooth surface due to self shadows. Atzberger (2000) simulated the influence of soil roughness on reflectance by using the SOILSPEC model. He found that, when the soil becomes smoother, due to decreasing micro-shadow effects, soil reflectance increases throughout the visible range.

Geometrical models have been developed to simulate bidirectional reflectance of light from rough soil surface based on the assumption that reflection is strongly correlated with the area of shadowed soil as well as on illumination and viewing geometry. Even though these models have been validated (Cierniewski, 1987; Cierniewski and Verbrugghe, 1997) their application in field conditions is not trivial, since many input parameters have to be considered which are quite difficult to assess in practical cases.

Several geometrical models (Cierniewski and Verbrugghe, 1994; Cooper and Smith, 1985; Irons et al., 1992; Norman et al., 1985) predict soil reflectance based on the assumption that shadowing of soil aggregates or clods has a greater influence than the scattering properties of a soil (Cierniewski and Verbrugghe, 1997). This study is also based on this principle and therefore **the influence of roughness on soil reflectance is estimated by assessing its shadowing effects**. This approach has been recently validated by (García Moreno et al., 2008).

The **purpose of this study** is to propose a new method to identify and reduce the effect of soil Relative Shadow (RS, the percentage of shadowed soil of the studied surface) on the assessment of SOC content from VNSWIR hyperspectral (350-2500 nm) field and airborne spectroscopic data.

First a method to measure RS and to correct its impact on field reflectance, measured with an Analytical Spectral Devices (ASD) spectroradiometer and the Airborne Hyperspectral Sensor (AHS), is proposed. Secondly the impact of RS on reflectance and SOCa accuracy is studied under laboratory conditions. Then SOC content is predicted by using uncorrected and corrected field reflectance values to evaluate the improvement in SOCa accuracy achieved with this method. The proposed method is finally compared with well-known mathematical **pre-processings** that intend to enhance SOCa accuracy.

2. DATA COLLECTION

2.1. Field data collection

2.1.1. Study area

The study area consisted of a north-south transect of ~7 km width and ~60 km length (NW corner: 50°03'N 6°03'E; SE corner: 49°33'N 6°12'E), crossing 4 of the 5 agro-geological regions of the Grand-Duchy of Luxembourg.

The Grand-Duchy of Luxembourg is characterised by a large variability of soils on a relatively small area (2586 km^2). The 4 agro-geological regions in the study area are:

- **The North**, called **Ardennes or Oesling**, is a relatively homogeneous area consisting of plateaus and dissected valley lying on a Devonian slate substrate. The Oesling presents soils that tend to accumulate organic matter with an average SOC content of 26 g C kg^{-1} (Lioy et al., 2007). The predominant soil types are Leptosols or dystric Cambisols according to the World Reference Base classification (FAO, 1998) with a sandy or sandy-loam texture.
- **The South of Luxembourg,** called **Gutland**, is characterised by a very diverse pedological context with several types of soils and a large SOC variability. The average SOC content in Gutland is 17 g C kg^{-1} (Lioy et al., 2007). This region can be further subdivided into 3 agro-geological zones:
  - **Minette**, in the south-western part presents relatively homogeneous soil conditions. Soils in this region are heavy with high clay content (clay or loam-clay texture) and with a predominance of Gleyic Luvisols and Vertisols.
  - The predominant geologic substrate of the **Middle of land** is Luxembourg sandstone. The texture of the soils in this area is nevertheless not only sandy, but also sometimes clay rich. The most common soils in this area are Arenosols and Cambisols.
  - **Redange region**, lying between the central part of Luxembourg and the Oesling, is characterised by a very heterogeneous geology. Within this area, red sandstone, limestone, loess, gypsum-keuper and others substrates are found. Texture is also variable but loam soils are predominant. Major soil types limited to the investigated area are Luvisols.

2.1.2. Field campaign

The field campaign took place on the 5th-6th October 2007. This time period was selected to ensure a high proportion of bare soils after harvest and ploughing of mainly maize fields. The weather conditions were lightly cloudy sky on the 5th October 2007 and perfect clear sky on the 6th of October 2007.

A total of 165 sampling plots were delimited in 22 bare fields (6 to 23 plots per field) evenly distributed in the 4 aforementioned agro-geological regions (5-6 fields by agro-geological region). Each sampling plot consisted of a 7.5 m wide square centred on a geographical position recorded by a GPS receiver in differential mode (localisation accuracy < 0.5 m).

For each plot, vertical digital photographs of the soil were taken for soil shadow analysis and several soil samples were collected for analysis of SOC content, soil moisture and soil surface spectral characteristics. Bulk soil samples (200g) were collected from the soil surface of each plot for further spectral analysis in the laboratory (Cf. section 2.2).

2.1.3. Soil Organic Carbon (SOC)

Each soil samples used for SOC analyses was composed of 10 sub-samples collected to a depth from 0 to 5 cm with an auger at random locations within the sampling plot. Soil organic carbon of air-dried and sieved (2 mm) samples was analysed by dry-combustion with a LECO CN analyser. Samples with

carbonates (detected using effervescence to 1 M HCl) were removed from the dataset. SOC contents varied from 7 to 40 g C kg^{-1} and differed markedly between soil types and agrogeological regions.

2.1.4. Soil moisture

The total amount of rainfall during the previous 7 day period before the over flight was 23.2 mm at an average air temperature of 10.3°C (Luxembourg City). Last rainfall events occurred 3 days before the field campaign. Gravimetric soil surface moisture was determined for 159 arbitrarily-selected soil samples taken the day of the over flight within the sampling plots in the very first millimetres of the soil surface (up to 1 cm) as presented in Stevens et al. (2010). Soil moisture content was relatively low and varied greatly according to soil type (median: 5.9%, range: 0.9–19.1%). This enabled to consider the soil surface as dry during the field campaign and, consequently, soil moisture was not considered as a factor affecting the soil reflectance in this study.

2.1.5. Soil shadow

Soil Relative Shadow (RS, the percentage of shadowed soil of the studied surface) was measured for each sampling plot from digital photographs of the soil surface taken vertically at nadir position and at 1.50 m high, during the day before the flight (05/10/2007) and the day of the flight, mainly with a Canon Power Shot A620 ® digital camera but also with a Canon DIGITAL IXUS 500 ® and a NIKON D50 ®. Each photograph was recorded as a composition of the 3 Red, Green and Blue (RGB) spectral bands. 3 photographs were taken within each sampling plot, with the sun in front of the operator and before other measurements (SOC, water content) in order to capture a non disturbed soil surface (neither operator's shadow nor footprint). Around 500 vertical soil photographs were taken on the 5th and 6th October (250/250). Photographs were taken simultaneously (in a time interval of maximum 10 min) with field ASD spectroradiometer measurements in order to have same illumination and consequently the same shadow conditions for both measures.

Photographs of soil were then analysed with the image analysis software DEFINIENS DEVELOPER 7.0 (DEFINIENS Inc., Munchen, Germany) through classical segmentation-classification process (Figure 1 a-b) in order to extract different variables. The segmentation was realised with the "Multiresolution-segmentation" algorithm that segments an image in spectral objects by locally minimizing their average spectral heterogeneity (DEFINIENS, 2007). Tests have been realised to find the parameters of this algorithm that are best for discriminating shadowed from illuminated soil surface. The following parameters were found appropriate for the segmentation of the digital photographs: weight = 1 for all 3 RGB spectral bands, "scale" = 75, "shape" = 0.1 and "compactness" = 0.9. The resulting spectral objects were classified in 2 classes only: "Illuminated Soil" and "Shadowed Soil". No distinction was made for objects with different light or shadow intensities. Membership functions used for the definition of these 2 classes were defined with the single object feature "Brightness". Brightness, computed for an image object, is defined as the sum of the mean values of the 3 RGB spectral bands, divided by their quantity (area) (DEFINIENS, 2007). The brightness threshold values defining the 2 classes did not overlap and were adapted depending on the photograph by visualising the mean brightness value of some soil objects at the spectral border of the 2 classes and by using the "Image Layer Histogram" tool as shown in Figure 1 c. RGB values of the 2 classes were clearly separable except for very few photographs where shadowed white stones were misclassified in the "Illuminated" class. Most of the time, the same brightness threshold value could be kept for all photographs of a field. For some fields, the impact of ploughed furrow direction on soil shadow can be seen on the photographs. Strong soil colour contrast was noticed inside some fields.

Then, classification statistics (Class, Area and Mean object value for the 3 RGB layers values) were exported into Matlab (Matworks Inc., Natick, USA) to compute the 3 parameters described below.

a b c

Figure 1 : (a) Greyscale vertical photograph of a ploughed bare crop field, (b) Classified photograph in "Illuminated" and "Shadowed" objects, (c) Histograms of pixel values [1 -256] of a soil photograph for the blue layer as given by the "Image Layer Histogram" tool of DEFINIENS software.

Soil Relative Shadow (RS), defined as the percentage of shadowed soil area on a photograph, has been computed according to equation 1.

$$RS_P = \frac{AS_P}{A_P} \qquad (1)$$

Where,

- RS_p, is the RS of the photograph P (%),
- AS_p, is the Area of Shadowed soil of the photograph P (in pixels)
- A_p, is the total Area of the photograph P (in pixels)

According to this procedure, the RS range encountered in the fields was **[0.28 to 0.68]** with a mean of 0.53, but usually observed RS were comprised in the range [0.4, 0.6].

The mean value of Definiens features "Mean Layer Value" of each of the 3 RGB spectral bands have been computed for the "Illuminated" class and for the entire photograph scene, for each photograph, according to equation 2 ("Illuminated" class) and 3 (entire photograph scene).

$$MFI = \frac{\sum_{i=1}^{nI}(A_i * F_i)}{A_I} \qquad (2)$$

Where,

- MFI, is the Mean Feature value for the "Illuminated" class of a photograph
- nI, is the number of objects belonging to the "Illuminated" class of a photograph
- A_i, is the area of the "Illuminated" object i in a photograph (in pixels)
- F_i, is the Feature value of the "Illuminated" object i in a photograph
- A_I, is the total Area of the "Illuminated" class of a photograph (in pixels)

$$MFSc = \frac{\sum_{i=1}^{nSc}(A_i * F_i)}{A_{Sc}} \qquad (3)$$

Where,

- $MFSc$, is the Mean Feature value for whole Scene of a photograph
- nSc, is the number of objects of the whole Scene of a photograph
- A_i, is the area of the object i of a photograph (in pixels)
- F_i, is the Feature value of the object i of a photograph
- A_{Sc}, is the total Area of a photograph (in pixels)

2.1.6. Field spectral measurement

2.1.6.1. Airborne Hyperspectral Sensor (AHS) measurement and pre-processings

The hyperspectral data cube was acquired with the Airborne Hyperspectral Sensor 160 (AHS) on the 6th October 2007, under a cloudless sky, with a spatial resolution of 2.6m * 2.6m. 5 hyperspectral images of 60 km long were acquired with a swath of 1.96 km and approximately 30 % of across track overlapping. Flight true heading was 175° and 355° and solar azimuth angle comprised between 155° and 188°. The AHS is a whiskbroom scanner characterised by a Field of View (FOV) of 90° and providing 63 spectral bands in the Visible, Near Infrared and Short Wave Infrared region of the electromagnetic spectrum (430 nm – 2540 nm). The AHS is configured to provide 20 bands with a Full Width at Half Maximum (FWHM) of 30 nm between 430 and 1030 nm (Visible and Near Infrared; VNIR), 42 bands with a FWHM of 18 nm between 1994 and 2540 nm (Short Wavelength Infrared; SWIR 2), complemented by an isolated band centred at 1600 nm with a FHWM of 90 nm (SWIR 1). At-sensor radiance data with corresponding geographical positions have been processed by the Central Data Processing Center of the Vlaamse Instelling voor Technologische Onderzoek (CDPC-VITO), which provided geometrically and atmospherically corrected at-surface reflectance values. The atmospheric and geometric corrections are described in Stevens et al. (2010). In short, the procedure consisted of (i) a geometric correction by means of direct georeferencing on a digital elevation model; (ii) an atmospheric correction with a modified version of the MODTRAN4 radiative transfer code using radiances and a grid containing positions and viewing geometry parameters; (iii) the re-sampling of atmospherically-corrected data.

Hyperspectral images of the flight lines were manipulated by using IDL language and ENVI software (ITT VIS, Boulder, CO). Spectral data of the 165 sampling sites were extracted from their corresponding positions in each image. When a plot was measured twice due to overlapping of neighbouring images the spectrum with the lowest viewing zenith angle was kept.

2.1.6.2. Analytical Spectral Devices (ASD) spectral measurements

Reflectance in the spectral range 350-2500 nm was measured with a FieldSpec Pro spectroradiometer (ASDinc, Boulder, USA). The instrument is characterised by a Full Width at Half Maximum of 3 nm for the 350-1000 nm region (Ultraviolet, Visible and Near Infrared) and 10 nm for the 1000-2500 nm region (Near Infra Red and Short Wavelength Infrared). Measurements were realised at nadir with a bare ASD pistol with a FOV of 25° and at a height of approximately 1 m, resulting in a studied soil area of approximately 15 dm^2 (circle of 44 cm in diameter).

A total of 96 sampling plots were measured with the ASD the day before the flight (5th October 2007) under imperfect weather conditions (lightly cloudy sky) and the day of the overflight under perfect clear sky. Ten individual ASD spectra were taken randomly across each sampling plot and averaged to produce a plot representative spectrum. Reflectance was determined by reference to a Spectralon® panel.

2.2. Laboratory data collection: spectral measurement

Reflectance of prepared soil samples, collected during the field survey, was measured in the laboratory for different levels of RS. Purposes of these measurements were to study the impact of RS on reflectance and SOCa accuracy and to compute correcting factor for RS by measuring reflectance in shadowed and reference (no shadow) conditions.

2.2.1. Material and soil sample

Reflectance measurements were realised in a darkroom. Air dried soil samples were illuminated with one "Lowel-pro light"® lamp (P2-10CE Dedicated CE approved 230v Euro model) with bulb of type GLF P44, which provides a stable light. The lamp zenith angle was 30 °. Bare ASD pistol was fixed at

the nadir of the soil sample, at a height of 22.6 cm, with FOV of 25 °, resulting in a studied soil area of 79 cm².

Soil samples collected during the field survey were used to prepare 96 soil samples belonging to 22 fields with, most of the time, 5 replicates per field. As surface roughness and particle size affects the albedo (Bishop et al., 1994; Whiting et al., 2004) soil material smaller than 2 mm in size was separated by sieving the air-dried samples after a light grinding with mortar and pestle. Coarse gravels and small stones, greater than 5 mm in size, were removed in the field, along with recognizable crop residue (in compliance with (Whiting et al., 2004). Each soil sample was composed of 20 g of these fine air dried soil fraction uniformly placed in a big plastic Petri dish (1, 20 mm deep, 145 mm in diameter) in a thin layer of 3 mm of soil.

2.2.2. Shadow modelling

Shadow was applied on the soil sample with the help of a calibrated sliding matte, placed between the light source and the soil sample. Seven predefined RS levels were: 0% (full light), 10, 28, 39, 60, 88 and 100% (full shadow) of the soil sample's area. Level 0 was the reference. Levels 0.28, 0.39 and 0.60 were selected to be close to the RS range met in field ([0.28 to 0.68]). Note that the intensity of the shadow was stronger in laboratory than in field because of the absence of the light diffuse component in the laboratory.

2.2.3. ASD spectral measurements

For each sample and shadow level, 3 spectral measurement replicates were taken by rotating the sample by 120° in order to take into account the reflectance variability due to surface geometry of soil sample.

3 post processings were further applied to measured spectra.

- Splice correction of the ViewSpecPro software ®, which corrects for the steps between the ASD sensors at 1000 nm and 1800 nm.
- Smoothing by using the Savitzky-Golay filter with the following parameter: odd filter length: 47; filter order: 3; no derivative of the filter coefficients (with R software; (R Development Core Team, 2009)).
- Average of the 3 spectra replicates (with R software).

Finally, in order to get laboratory spectra at exactly the same RS level as the one observed in the field for each soil sample, the series of seven laboratory ASD measurements of each soil sample were used to interpolate spectra at the field RS level, with a cubic spline function.

3. METHOD

The logic of the method aiming at enhancing SOCa by reducing RS effect is described below and consists of 4 steps:

1. Computing shadow correction factors "K" for field reflectance from collected data
2. Correcting field reflectance (ASD and AHS) with the "K" produced
3. Estimating whether corrected reflectance improve SOCa
4. Comparing the performance of the proposed correction method with existing methods

The global workflow of this study is presented in the Figure 2 (steps 1-3).

3.1. Computation of shadow correction factors in the visible range (K_{VIS})

Soil photographs taken during the field campaign and derived parameters (Cf. section 2.1.5) were used to compute the RS correction factors in the visible range "$\mathbf{K_{VIS}}$" for each soil sample.

K_{VIS} expresses the percentage of "reflectance" – of a photograph, AHS or ASD spectrum - of a shadowed scene that has to be added to that shadowed reflectance to get the non-shadowed reflectance value.

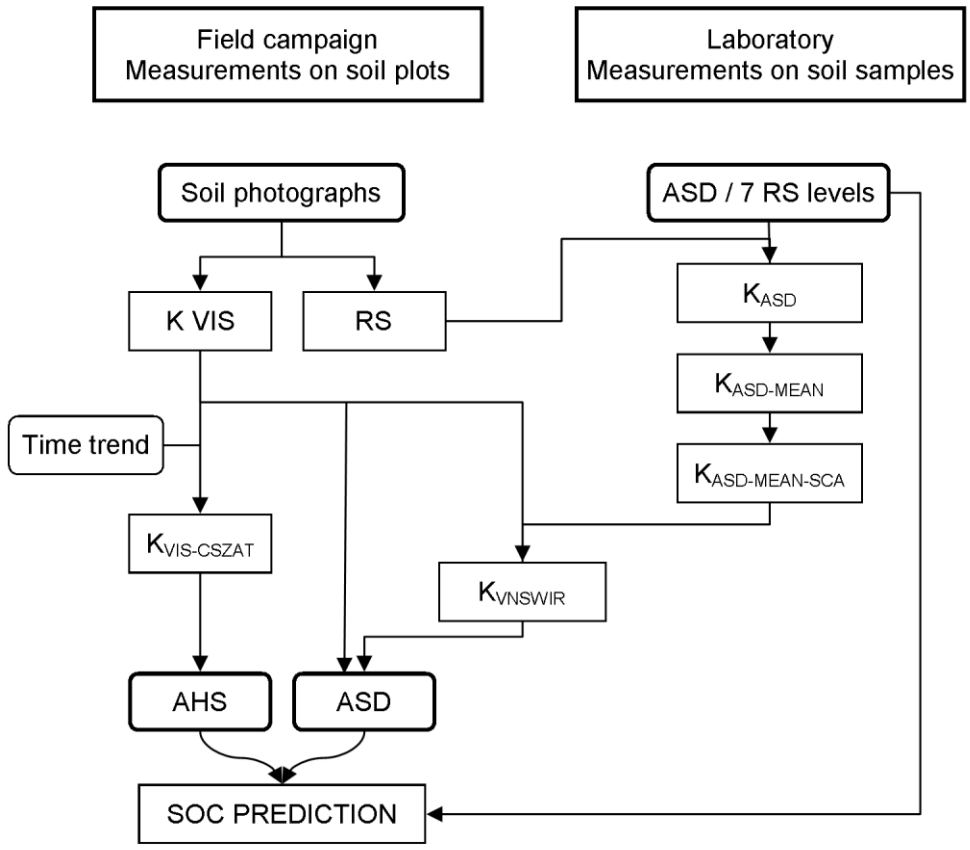

Figure 2: Global workflow of this study

The RS correction factors for the aforementioned Definiens Features **"Mean Layer Value"** of the 3 RGB layers have been computed according to the equation 4, resulting in the 3 "$\mathbf{K_{RGB}}$": K_{Red}, K_{Green}, K_{Blue}.

$$K_{RGB} = \frac{(MFI - MFSc)}{MFSc} \quad (4)$$

Where,

- K_{RGB}, is the "RGB" shadow correction factor for a given Definiens Feature (%)
- *MFI*, is the Mean Feature value for the Illuminated class of a photograph (Digital Number [1 - 256])
- *MFSc*, is the Mean Feature value for the whole Scene of a photograph (Digital Number [1 - 256])

The mean of the 3 correction factors K_{Red}, K_{Green} and K_{Blue}, corresponding to the mean K in the visible spectral range ($\mathbf{K_{VIS}}$) (equation 5), was computed for each photograph.

$$K_{VIS} = \frac{(K_{Red} + K_{Green} + K_{Blue})}{3} \quad (5)$$

As K_{Red}, K_{Green}, K_{Blue} and K_{VIS} were highly correlated (e.g. R^2 of K_{Red} and K_{Green} is higher than 0.95), only K_{VIS} values were further used in this study. Mean value of K_{VIS} by sampling plot (3 photographs per plot) were then computed.

The correction of a field reflectance disturbed by RS (photograph, ASD or AHS spectrum) was then realised as indicated in equation 6 below.

$$R_{fcor} = R_f * (1 + K_{VIS}) \quad (6)$$

Where,

- R_{fcor}, is the field reflectance (photograph, AHS or ASD) corrected for RS effect
- R_f, is the observed field reflectance (photograph, AHS or ASD)

The **main hypothesis** is that K_{VIS} can be applied on ASD and AHS reflectance in the purpose of RS effect correction and consequently that the 2 following equations are verified:

$$R_{ASD\_ref} = R_{ASD\_RS} * (1 + K_{VIS})$$
$$R_{AHS\_ref} = R_{AHS\_RS} * (1 + K_{VIS})$$

Where,

- R_{ASD_ref} and R_{AHS_ref}, are ASD or AHS reflectance for a non-shadowed soil
- R_{ASD_RS} and R_{AHS_RS}, are ASD or AHS reflectance for a shadowed soil

In particular the AHS sensor viewing angle has not been taken into consideration in this study. Note also that the Field Of View (FOV) of the RGB cameras (50°) is twice wider than the one of the ASD spectrometer (25°) and nearly twice narrower than the one of the AHS (90°). This difference has not been taken into account for the computation of the correction factors and their application on the field ASD and AHS reflectances.

3.1.1. K_{VIS} time trend correction

3.1.1.1. RS and K_{VIS} time trend

The analysis of RS and K_{VIS} as a function of time during the data collection in the fields revealed that a strong time trend affects RS as illustrated in Figure 3 but also to a smaller extent K_{VIS}. RS and K_{VIS} were smaller at midday and higher in the morning and afternoon periods. This time trend is caused by Solar Zenith Angle (SZA) variations during the day, as suggested by the fact that R^2 between all 165 observed RS and SZA is 0.64 with a 2nd degree polynomial, and 0.98 between RS trend and SZA.

These observations lead to the conclusion that the time of the photo acquisition has a strong influence on RS values. This effect is probably even more important that the RS variation due to difference in roughness between plots or fields.

3.1.1.2. K_{VIS} time trend correction

Considering this strong time trend and the fact that most of the photographs were not taken simultaneously with the AHS flight, it appeared necessary to correct K_{VIS} for the time trend before applying it to AHS spectra.

This time trend correction was realised, in a first step, by assigning to each plot the time of the mid-flight lines (a flight line lasted 13 min) of the AHS image from which its AHS spectrum was extracted. Maximum time error is thus 6.5 min for each plot. Secondly, the time scale was transformed into a SZA scale in order to get a physical basis to the trend and K_{VIS} was expressed as a function of SZA.

The Trend of K_{VIS} according to SZA is called K_{VIS} SZAT. Then the values of the K_{VIS} SZAT at the time of the AHS flight over each plot and at the time when photograph was taken in each plot were extracted and used to compute the detrended K_{VIS} according to the equation 7.

$$K_{VIS\_CSZAT} = K_{VIS} + \left(K_{AHS\_SZAT} - K_{VIS\_SZAT}\right) \quad (7)$$

Where,

- $K_{VIS\text{-}CSZAT}$, is the K_{VIS} Corrected from the SZA Trend as if K_{VIS} was measured at the AHS flight time over the plot (%)
- K_{VIS}, is the K_{VIS} value observed in the plot (%)
- $K_{AHS\text{-}SZAT}$, is the K_{VIS} value extracted from the K_{VIS} SZA Trend at the time of AHS flight over the plot (%)
- $K_{VIS\text{-}SZAT}$, is the K_{VIS} value extracted from the K_{VIS} SZA Trend at the time of the K_{VIS} observation in the plot (%)

No trend corrections were applied to the K_{VIS} to be applied on ASD field reflectance, since ASD reflectances were taken simultaneously with the digital photo.

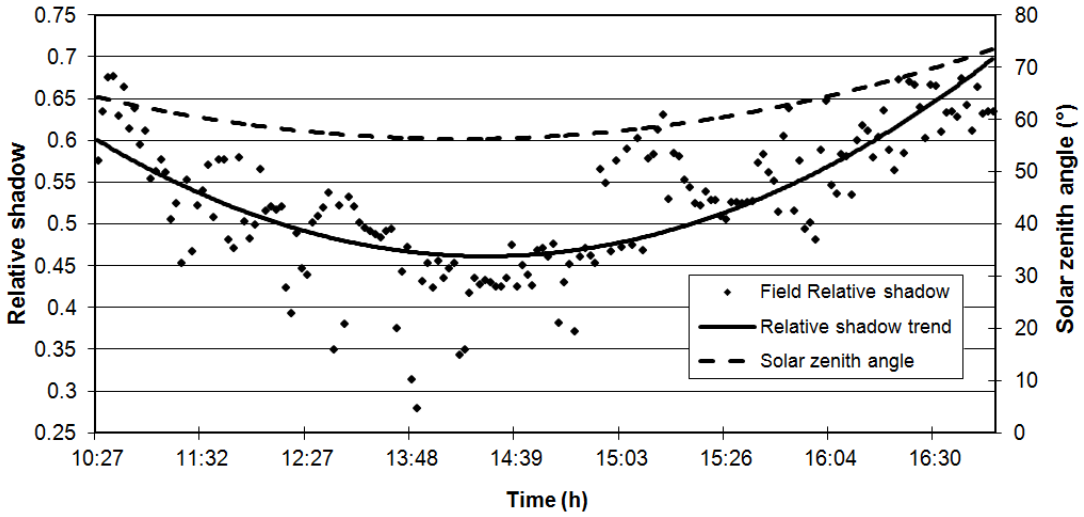

Figure 3 : RS temporal evolution for all 165 soil sampling plots, RS time trend and solar zenith angle evolution on the 6th October 2007, on the study site (49.80° latitude – 6.13° Longitude).

3.2. Computation of shadow correction factors in the range [350-2500 nm] (K_{VNSWIR})

Each K_{VIS} is composed of a single value computed in the visible, and consequently the correction of an ASD reflectance spectrum (covering the spectral range 350-2500 nm) with such a K_{VIS} consists of a simple multiplication of each spectral bands by a single K_{VIS} value (equation 5). As laboratory experiments showed that the influence of soil RS on reflectance is not wavelength-independent (Figure 4), correction factors covering the full VIS-NIR-SWIR spectral range were needed and were computed from laboratory ASD spectra measured in full light and at the RS level met in the field. The computation of these correction factors consisted of the 3 following steps.

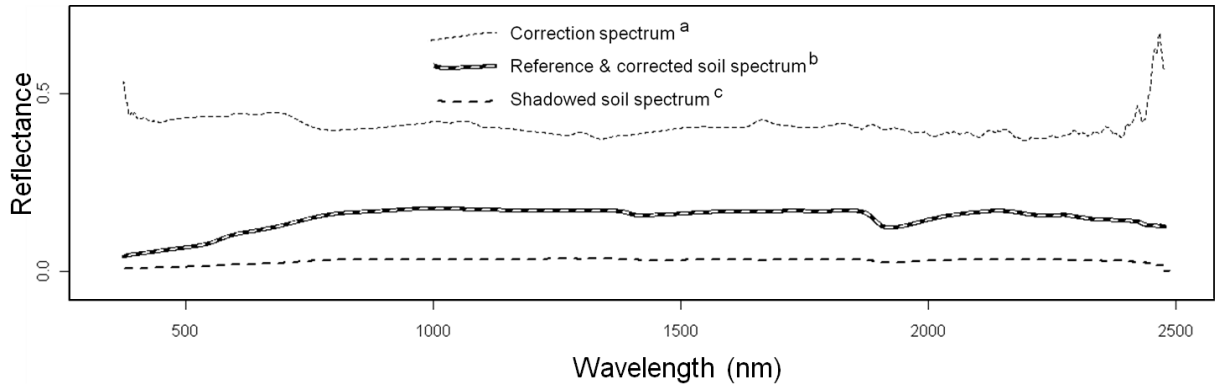

Figure 4 : Soil shadow correction spectrum: a) typical shape of a K_{ASD} (K_{ASD}/10); b) the reference (non-shadowed) ASD spectrum & the shadowed spectrum corrected with the K_{ASD} ; c) the ASD spectrum of a shadowed soil sample

3.2.1. Computation of the ASD correction spectra (K_{ASD})

First, for each laboratory soil sample, a K_{ASD} is computed based on the laboratory ASD spectrum measured in full light and at the RS level met in the field for the considered soil sample as indicated in equation 8.

$$K_{ASD} = \frac{\left(R_{ASD\_0} - R_{ASD\_f}\right)}{R_{ASD\_f}} \quad (8)$$

Where,

- K_{ASD}, is a correction factor spectrum in the spectral range [350-2500 nm]
- R_{ASD_0}, is the laboratory ASD reflectance spectrum measured under full light (no shadow)
- R_{ASD_f}, is the laboratory ASD reflectance spectrum measured at the RS level met in the field

Figure 4 presents a typical correction factor spectrum (dotted black (a)) computed from ASD laboratory reflectance. This figure shows clearly that the influence of RS varies with wavelength. The K_{ASD} correction is applied to an observed spectrum similarly to the K_{VIS} correction (equation 5).

3.2.2. Computation of the arithmetic mean of all K_{ASD} ($K_{ASD\text{-}MEAN}$) and scaling ($K_{ASD\text{-}MEAN\text{-}SCA}$)

In order to get a single reference correction spectrum shape, the arithmetic mean of the K_{ASD} of all soil samples was computed ($K_{ASD\text{-}MEAN}$). Then this K_{ASD_MEAN} was scaled in order for the "visible" (at 585 nm) part of the resulting spectrum ($K_{ASD\ MEAN\ SCA}$) to be equal to 1 (equation 9). The wavelength of 585nm was chosen as reference for the visible range since it was the part of the visible spectra that presented the least variation.

$$K_{\text{ASD MEAN SCA}} = \frac{K_{ASD\_MEAN}}{K_{ASD\_MEAN\,585nm}} \quad (9)$$

Where,

- $K_{ASD\ MEAN\ SCA}$, is the scaled K_{ASD_MEAN}
- K_{ASD_MEAN}, is the arithmetic mean of all K_{ASD}
- $K_{ASD\_MEAN585nm}$, is the K_{ASD_MEAN} value at 585 nm

3.2.3. Extending K_{VIS} in the range [350-2500 nm] (K_{VNSWIR})

Finally $K_{ASD\ MEAN\ SCA}$ is used to extend the K_{VIS} values in the [350-2500 nm] spectral domain by simple multiplication (equation 10). The resulting correction factors are subsequently referred to as $\mathbf{K_{VNSWIR}}$ (K in the Visible, Near and Short-Wave Infrared).

$$K_{VNSWIR} = K_{VIS} * K_{ASD\_MEAN\_SCA} \quad (10)$$

Where,

- K_{VNSWIR}, are the extended K_{VIS} in the range [350-2500 nm] (Visible, Near and Short-Wave Infrared)
- K_{VIS}, are the K_{VIS} single value
- $K_{ASD\ MEAN\ SCA}$, is the scaled mean hyperspectral K_{ASD}

As a result, K_{VNSWIR} keeps the original K_{VIS} value at 585 nm while the rest of the correction factor results from the multiplication of the original K_{VIS} by the $K_{ASD\ MEAN\ SCA}$.

Note that it is supposed here that the effect of shadow on reflectance is the same or similar in the field and in laboratory what allows the construction of correction spectra in laboratory and their application on field reflectance. This hypothesis could not be checked since any reference reflectance (non-shadowed) could be measured in the fields. Moreover, shadow modelling in laboratory is probably not perfect and lightning conditions in and outdoor differ (sun versus lamp).

3.3. Field reflectance correction

Field reflectances were corrected by applying the previously created correction factors as indicated in the equation 11, with K representing the different correction factors according to sensors and wavelength ranges (K_{VIS} or K_{VNSWIR}), and "Reflectance" referring to field ASD or AHS reflectance.

$$Corrected\ Reflectance = Field\ reflectance * (1 + K) \quad (11)$$

Field ASD reflectances were corrected with the non detrended correction factor since photographs and ASD measures were recorded simultaneously. K_{VIS} and K_{VNSWIR} were applied on 96 field ASD reflectances. AHS reflectances were corrected with detrended K_{VIS} for 165 soil samples. The K_{VNSWIR} were not tested on AHS reflectance.

3.4. SOCa method description

SOCa was performed by means of Partial Least Square Regression (PLSR) under leave-one-out cross-validation. The performance of the assessment model was measured by the Root Mean Square Error of Assessment in Cross Validation (RMSECV) and by the Ratio of Performance to Deviation (RPD, the ratio between standard deviation and RMSECV). Statistical manipulations were carried out with the R software (R Development Core Team, 2009) and, in particular, with the PLS package of Wehrens and Mevik (2007). The details of the calibration procedure can be found in Stevens et al.(2010).

3.5. Estimation of SOCa accuracy enhancement

In order to estimate whether field reflectance (ASD and AHS) correction improves SOCa accuracy, SOCa was realised with both **uncorrected** and **corrected** field reflectance. RPD and RMSECV were compared.

The ability to enhance the SOCa accuracy of the "K-correction method" described above was finally compared to the one of well-known mathematical **pre-processings** that intend to decrease the noise of

the spectral signal, enhance possible spectral features linked to the property studied and correct for light scattering effects. These pre-processings are (i) conversion to absorbance (-logR), (ii) 1st and 2nd derivatives, (iii) 1st and 2nd gap derivatives (Norris and Williams, 1984), (iv) Savitzky-Golay smoothing and derivatives (Savitzky and Golay, 1964), (v) Whittaker smoothing (Eilers, 2003), (vi) detrending (Barnes et al., 1989), (vii) Multiplicative Scatter Correction (Geladi et al., 1985), (viii) a combination of the previous. All pre-processings were systematically tested on field reflectance and only the best one in terms of RPD value of the SOCa was retained for comparison with the K-correction method.

4. RESULTS

4.1. Impact of soil Relative Shadow (RS) on reflectance and Soil Organic Carbon assessment (SOCa) accuracy based on laboratory data

Figure 5 shows the reflectance decrease with increasing RS on one soil sample studied under laboratory conditions. Table 1 presents the impact of RS on SOCa accuracy. Generally increasing soil RS decreases SOCa accuracy. In particular the range of RS measured during the field campaign, as modelled in laboratory, decreases SOCa accuracy significantly. An increase of 20 % of RMSECV is observed for the SOCa realised under the field RS range (RMSECV of 3.75) compared to the one realised under full light condition (no shadow) (RMSECV of 3.12). No pre-processing, except those mentioned in section 2.2.3, was tested on laboratory ASD reflectance for improving SOCa. These results justify the need for a correction of shadowing effect on field soil reflectance.

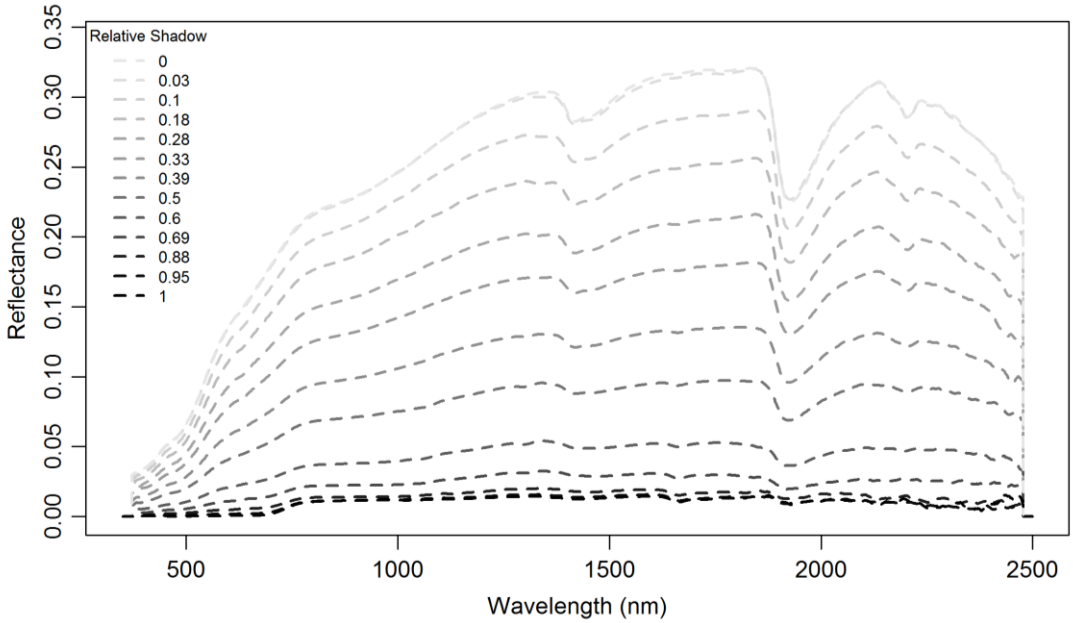

Figure 5 : Reflectance spectra of a sandy loam soil sample for 13 Relative Shadow levels measured under laboratory condition at a soil moisture level of 0.05.

Table 1 : SOCa accuracy for 52 soil samples analysed in laboratory for different RS conditions.

Relative Shadow	RMSECV [a]	RPD [b]	N [c]
0	3.12	3.07	52
0.20	3.26	2.94	52
0.50	3.53	2.72	52
0.88	4.19	2.28	52
1	5.35	1.79	52
Field value [d] [0.28, 0.68]	3.75	2.56	52

[a] RMSECV, the Root Mean Square Error in Cross-Validation expressed in gC/kg dry soil
[b] RPD, the Ratio of Performance to Deviation
[c] N, the number of soil samples
[d] Field value, the range of values measured during the field campaign. In this case the RS level applied on each laboratory soil sample is the RS level measured during the field campaign on the corresponding soil sample

4.2. SOCa accuracy enhancement for corrected field reflectance

For each type of spectral field measurement (ASD, AHS), SOCa is presented first for non-pre-processed uncorrected and K-corrected reflectance and secondly for pre-processed (cf. section 3.5) uncorrected and K-corrected reflectance. Only the pre-processing giving the best SOCa results in terms of RPD is presented.

4.2.1. SOCa accuracy enhancement for corrected ASD field reflectance

Results presented in Table 2-T1 show that both K_{VIS} and K_{VNSWIR} correction methods improve significantly both RPD and RMSECV values of SOCa. In particular, SOCa enhancement is 10 % RMSECV with K_{VIS} and 27 % RMSECV with K_{VNSWIR}.

Table 2-T2 presents the SOCa results obtained with the pre-processed ASD reflectance. Compared to non-pre-processed uncorrected reflectance, pre-processings alone enables a SOCa accuracy enhancement of 25 % RMSECV and the total enhancement reaches 27% and 29 % RMSECV for the correction combining pre-processings and K_{VIS} and K_{VNSWIR} respectively. The best SOCa is obtained with the pre-processed reflectance (conversion into absorbance) corrected with K_{VNSWIR}.

The SOCa accuracy enhancement is 3 and 5 % RMSECV with K_{VIS} and K_{VNSWIR} respectively applied on pre-processed reflectance compared to the SOCa result obtained with the pre-processed uncorrected reflectance. The fact that the SOCa enhancement is significantly smaller when the K-correction method is combined with pre-processings suggests that an important part of the shadow disturbing effect is corrected by both methods.

The K_{VNSWIR} correction factor seems to be the most useful since it gives the best SOCa with or without pre-processings. In particular, when using non pre-processed reflectance, the SOCa enhancement obtained by K_{VNSWIR} is much larger than the one obtained by K_{VIS} (18 % RMSECV).

The fact that the best K-correction (K_{VNSWIR}) on non-pre-processed reflectance gives better SOCa than the best pre-processing on uncorrected reflectance suggests that the proposed K-correction method is relevant for correcting field ASD reflectance and is better than present pre-processings.

4.2.2. SOCa accuracy enhancement for corrected AHS field reflectance

A set of 91 AHS spectra were corrected by using $K_{VIS\ CTSZA}$ computed from photographs taken the day of the flight (06/10/2007) only. Results presented in Table 2-T3 show that $K_{VIS\ CTSZA}$ correction method improves significantly both RPD and RMSECV values of SOCa (enhancement of 25 % RMSECV) for AHS spectra.

Table 2-T4 presents the SOCa results obtained with the pre-processed AHS reflectance. Compared to non-pre-processed uncorrected reflectance, pre-processings alone enables a SOCa accuracy enhancement of 20% RMSECV and the total enhancement reaches 25% RMSECV for the correction combining pre-processings and $K_{VIS\ CTSZA}$. The best SOCa is achieved using $K_{VIS\ CTSZA}$-corrected and pre-processed reflectance.

The SOCa accuracy enhancement is 6 % RMSECV with $K_{VIS\ CTSZA}$ applied on pre-processed reflectance compared to the SOCa result obtained with the pre-processed uncorrected reflectance. Here also it can be concluded that an important part of the shadow disturbing effect is corrected by both methods.

The fact that the $K_{VIS\ CTSZA}$ correction method on non-pre-processed reflectance (RPD of 3.13) gives better SOCa than the best pre-processing on uncorrected reflectance (RPD of 3.07) suggests that the

Table 2 : SOCa accuracy in outdoor conditions for the different sensors, pre-processings and K-correction factors

Ref. Text [a]	Sensor [b]	Preprocessing [c]	K-correction [d]	RPD [e]	RMSECV [f]	R^2 [g]	N [h]	SD [i]	SOCa Enh./pp [j]	SOCa Enh./non-pp [k]
T1	ASD	No	No	2.51	4.42	0.77	96	11.08	/	/
			K_{VIS}	2.81	3.96	0.83	96	11.13	/	10
			K_{VNSWIR}	3.4	3.24	0.89	96	11.04	/	27
T2	ASD	Absorbance	No	3.33	3.31	0.89	96	11.04	/	25
		$SG_{R.0.4.5}$	K_{VIS}	3.45	3.21	0.9	96	11.08	3	27
		$SG_{R.0.3.21}$	K_{VNSWIR}	3.53	3.13	0.91	96	11.04	5	29
T3	AHS	No	No	2.4	4.9	0.93	90	11.75	/	/
			$K_{VIS\ CTSZA}$ [l]	3.13	3.68	0.96	91	11.52	/	25
T4	AHS	SG.R.2.4.11	No	3.07	3.92	0.96	88	12.05	/	20
		Reflectance	$K_{VIS\ CTSZA}$ [l]	3.13	3.68	0.96	91	11.52	6	25

[a] Ref. text, the reference notation to the text
[b] Sensor, the type of sensor used: ASD: Analytical Spectral Devices or AHS: Airborne Hyperspectral Sensor.
[c] Pre-processing, the pre-processing giving the best SOCa. SG_R stands for a Savitzky–Golay smoothing filter applied on reflectance. The 3 subscript numbers are the 3 SG parameters: differentiation order, polynomial order and frame size
[d] K-correction, the K-correction factor used
[e] RPD, the Ratio of Performance to Deviation
[f] RMSECV, the Root Mean Square Error in Cross-Validation expressed in gC/kg dry soil.
[g] R^2, the coefficient of determination
[h] N, the number of soil samples
[i] SD, the Standard Deviation
[j] SOCa enhancement compared to pre-processed uncorrected reflectance expressed as percentage of RMSECV
[k] SOCa enhancement compared to non-pre-processed uncorrected reflectance expressed as percentage of RMSECV
[l] $K_{VIS\ CTSZA}$ is computed from photographs taken the day of the flight only (6th October 2007)

proposed method is relevant also for correcting field AHS reflectance and is slightly better than the existing pre-processings.

The correction of a dataset of 165 AHS spectra with K_{VIS} computed from photographs taken the day of the flight and the day before the flight leads to the same general conclusions than above. In view of these results, applying a K_{VNSWIR} to AHS reflectance should give good results but this could not be done in this study due to lack of time.

4.2.3. Comparison of SOCa accuracy for corrected ASD and AHS field reflectance

In terms of **RPD absolute value**, as expected, SOCa from pre-processed ASD corrected with K_{VIS} (RPD of 3.45) presents a better accuracy than the SOCa from AHS with the same treatment (RPD of 3.13). This is in line with the results of Stevens et al. (2008) who also found that SOCa from field ASD is more accurate than the one with AHS. This can be explained by the fact that the ASD has a higher radiometric resolution with 2151 spectral bands versus 63 only for AHS, that the AHS signal is highly disturbed by the atmosphere and that the AHS viewing angle varies for each soil sample whereas it is always the same for ASD. Consequently better SOC predictors may be found with ASD.

In terms of **SOCa accuracy enhancement** measured in % of RMSECV, the SOCa enhancement is double or more for AHS compared to ASD data. Indeed, for non-pre-processed reflectance corrected with K_{VIS} SOCa enhancement is 10 % RMSECV for ASD and 25 % for AHS. For pre-processed reflectance corrected with K_{VIS}, supplementary SOCa enhancement enabled by the K-correction method is 3 % RMSECV for ASD and 6 % for AHS.

5. DISCUSSION AND CONCLUSION

This study is based on the idea that the soil shadow, which is due to soil roughness in field conditions, decreases the accuracy of the SOCa from soil reflectance. This has been confirmed by laboratory experiments that showed that **the accuracy of SOCa from prepared soil samples decreases when the RS level applied on these soil samples increases**. As a result the purpose of this study was to find a method that reduces the RS effect on soil reflectance in order to enhance SOCa.

A **new method** for identifying and correcting the effect of soil RS on field reflectance spectra measured with an ASD and AHS during field campaign was elaborated and tested. This method is based on the acquisition of digital photographs of the soil surface in the visible range and the derivation of a shadow correction factor ($\mathbf{K_{VIS}}$) resulting from the comparison of the "reflectance" of shadowed and illuminated soil areas. Moreover, the study of laboratory ASD reflectance of shadowed soil samples showed that the influence of shadow on reflectance vary with wavelength and RS intensity. Consequently a correction factor in the entire [350 -2500 nm] spectral range was computed to take into account this differential influence ($\mathbf{K_{VNSWIR}}$).

Results showed that the **proposed method enables to improve significantly SOCa** by correcting the effect of soil relative shadow on both studied spectral data types (portable field and airborne spectrometry).

This method enabled to achieve **SOCa accuracy improvement** of 27 % RMSECV for ASD reflectance (with K_{VNSWIR}) and 25 % RMSECV for AHS reflectance (with K_{VIS}), where traditional methods (aforementioned as "pre-processings") enabled an enhancement of 25 % (ASD) and 20 % (AHS) RMSECV only.
Moreover the fact that this method enhances SOCa even on pre-processed (Cf. the "pre-processings", section 3.5) reflectance, suggests that the **proposed method enables to correct part of the shadow disturbing effect that existing pre-processing techniques can not take into account**.
Nevertheless the best SOCa are always achieved when combining pre-processings with the K-correction method proposed here.

The fact that the pre-processings technique gives nearly the same SOCa enhancement than the K-method, which is a method specially dedicated to the correction of the soil relative shadow, suggests that what is corrected by the pre-processings, beside the spectra noise, is predominantly the soil shadow effect.

The fact that the impact of RS does not affect all wavelengths in the same way suggests that it would be possible to find spectral features correlated with RS level. This would open the possibility to identify the RS levels from the fields hyperspectral measurement itself and consequently to apply a correction through a simple mathematical treatment. This is in line with the conclusions of Wu et al. (2009) who suggests that NIR could be used to estimate the soil roughness.

Beside the fact that the K_{VNSWIR} enhance significantly the SOCa seems to confirm that the **shadow disturbing effect for SOCa assessment is wavelength dependent**.

The proposed method has the **advantage** that the correction applied is directly related and proportional to the shadow level observed and take into account the wavelength dependence on RS, contrariwise to traditional pre-processings that are not related to a measured shadow level and use spectra transformation that are based on the idea that shadow effect is constant on the whole [350-2500 nm] range. Conversely this method presents the big **disadvantage** that precise information on the soil shadow level is needed in all points of the studied area and that the collection of this information is labour intensive and time consuming. An ideal solution would be to derive information on the relative shadow level from the reflectance spectra itself.

To the present knowledge and considering the easiness of application (mathematical transformation) and good efficiency of existing pre-processings to handle soil shadow disturbing effect (20 to 25 % RMSECV enhancement), the small supplementary SOCa enhancement that the K-correction enables compared to pre-processings (3 to 6 % RMSECV supplementary enhancement) and the considerable amount of work this method requires, it is advised to put more research effort in the finding of spectral mathematical treatments able to mitigate the effect of soil shadow and roughness on reflectance.

ACKNOWLEDGEMENTS

The research in this paper is funded by the Belgian Science Policy Office and the National Research Fund of Luxembourg in the framework of the STEREO II program – Project "Monitoring soil organic carbon in croplands using imaging spectroscopy" (SR/00/110). We thank also the Vlaamse Instelling voor Technologische Onderzoek (VITO) at Mol (Belgium) for the organization of the flight campaign and geometric/atmospheric corrections of the images and Damien ROSILLON who elaborated part of the method while working under the CARBIS project (contract number: SR/00/71).

REFERENCES

Arnfield, A.J., 1975. A note on the diurnal, latitudinal and seasonal variation of the surface reflection coefficient. Journal of Applied Meteorology, 14(8): 1603-1608.

Atzberger, C., 2000. Systematic evaluation of factors interfering with soil colour retrieval from space. . Proceedings 2nd EARSeL workshop on imaging spectroscopy, Enschede. International Institute for aerospace survey and earth sciences (ITC).

Barnes, R.J., Dhanoa, M.S. and Lister, S.J., 1989. Standard normal variation transformation and de-trending of near-infrared diffuse reflectance spectra. Applied Spectroscopy, 43: 772-777.

Bishop, J.L., Pieters, C. M., & Edwards, J. O. Clays and, 1994. Infrared spectroscopic analyses on the nature of water in montmorillonite. Clays and Clay Minerals, 42: 702-716.

Cierniewski, J., 1987. A model for soil surface roughness influence on the spectral response of bare soils in the visible and near-infrared range. Remote sensing of environment, 23: 97-115.

Cierniewski, J. and Verbrugghe, M., 1994. A geometrical model of soil bidirectional reflectance in the visible and near-infrared range. Proceedings of 6th International Symposium on Physical Measurements and Signatures in Remote Sensing, 17-2 January 1994, Val d'Isère, France: International Society for Photogrammetry and Remote Sensing, 17: 635-642.

Cierniewski, J., Verbrugghe, M., 1997. Influence of soil surface roughness on soil bidirectional reflectance. International journal of remote sensing, 18(6): 1277-1288.

Cooper, K.D. and Smith, J.A., 1985. A Monte Carlo reflectance model for soil surfaces with three-dimensional structure. I.E.E.E. Transations on Geoscience and Remote Sensing, 23: 668-673.

DEFINIENS, 2007. Definiens Developer 7. Reference Book, pp. 99 - 100.

Eilers, P.H.C., 2003. A perfect smoother. Analytical Chemistry, 75(6331-3636).

FAO, 1998. World Reference Base for Soil Resources. World Soil Resources Report, 84.

García Moreno, R., Saa Requejo, A., Tarquis Alonso, A.M., Barrington, S. and Díaz, M.C., 2008. Shadow analysis: A method for measuring soil surface roughness. Geoderma, 146(1-2): 201-208.

Geladi, P., MacDougall, D. and Martens, H., 1985. Linearization and scatter-correction for nearinfrared reflectance spectra of meat. Applied Spectroscopy, 39: 491-500.

Irons, J.R., Campbell, G.S., Norman, J.M., Graham, D.W. and Kovalick, W.M., 1992. Prediction and measurement of soil bidirectional reflectance. I.E.E.E. Transations on Geoscience and Remote Sensing, 30: 249-260.

Lioy, R. et al., 2007. Beurteilung der Versorgung Luxemburger landwirtschaftlicher Betriebe mit Schwefel, Calcium und Magnesium anhand der Hoftorbilanz. . VDLUFA-Schriftenreihe Bd. 63/2008, SS. : 711-720.

Norman, J.M., Welles, J.M. and Walter, E.A., 1985. Contrast among bidirectional reflectance of leaves, canopies, and soils. I.E.E.E. Transactions on Geoscience and Remote Sensing of Environment, 23: 659-667.

Norris, K.H. and Williams, P.C., 1984. Optimization of mathematical treatments of raw nearinfrared signal in the measurement of protein in hard red spring wheat. 1. Influence of particle size. Cereal Chemistry, 61: 158-165.

R Development Core Team, 2009. R: A language and environment for statistical computing. R Foundation for Statistical Computing, Vienna, Austria. ISBN 3-900051-07-0.

Savitzky, A. and Golay, M.J.E., 1964. Smoothing and differentiation of data by simplified leastsquare procedures. Analytical Chemistry, 36: 1627-1638.

Stevens, A. et al., 2010. Measuring soil organic carbon in croplands at regional scale using airborne imaging spectroscopy. Geoderma, 158(1–2): 32-45.

Stevens, A. et al., 2008. Laboratory, field and airborne spectroscopy for monitoring organic carbon content in agricultural soils. Geoderma, 144(1-2): 395-404.

Viscarra Rossel, R.A., Minasny, B., Roudier, P. and McBratney, A.B., 2006. Colour space models for soil science. Geoderma, 133(3–4): 320-337.

Wehrens, R. and Mevik, B.-H., 2007. PLS: Partial Least Squares Regression (PLSR) and Principal Component Regression (PCR). R package version 2.1-0.

Whiting, M.L., Li, L. and Ustin, S.L., 2004. Predicting water content using Gaussian model on soil spectra. Remote Sensing of Environment, 89(4): 535-552.

Wu, C.-Y., Jacobson, A.R., Laba, M. and Baveye, P.C., 2009. Accounting for surface roughness effects in the near-infrared reflectance sensing of soils. Geoderma, 152(1-2): 171-180.